Suppression of transient receptor potential melastatin 7 channel induces cell death in gastric cancer

Byung Joo Kim,[1] Eun Jung Park,[1] Jae Hwa Lee,[1] Ju-Hong Jeon,[1] Seon Jeong Kim[2] and Insuk So[1,3]

[1]Center for Bio-Artificial Muscle and Department of Physiology, Seoul National University College of Medicine, Seoul 110-799; [2]Center for Bio-Artificial Muscle and Department of Biomedical Engineering, Hanyang University, Seoul 133-791, Korea

(Received June 13, 2008/Revised August 11, 2008/Accepted August 14, 2008/Online publication November 20, 2008)

Ca^{2+} and Mg^{2+} have a fundamental role in many cellular processes and ion channels are involved in normal physiologic processes and in the pathology of various diseases. The aim here was to show that the presence and potential role of transient receptor potential melastatin 7 (TRPM7) channels in the growth and survival of AGS cells, the most common human gastric adenocarcinoma cell line. The patch-clamp technique for whole-cell recording was used in AGS cells. TRPM7-specific small interfering RNAs were used for specific inhibition of TRPM7. Whole-cell voltage-clamp recordings revealed the TRPM7-like currents that activated spontaneously following loss of intracellular Mg^{2+}. The current had a non-linear current–voltage relationship with the characteristic steep outward rectification associated with TRPM7 channels. Reverse transcription–polymerase chain reaction, western blotting, and immunoreactivity all showed abundant expression of TRPM7 messenger RNA and protein in AGS cells. Transfection of AGS cells with TRPM7 siRNA significantly reduced the expression of TRPM7 mRNA and protein as well as the amplitude of the TRPM7-like currents. Furthermore, we found that Mg^{2+} is critical for the growth and survival in AGS cells. Blockade of TRPM7 channels by La^{3+} and 2-APB or suppression of TRPM7 expression by siRNA inhibited the growth and survival of these cells. Human gastric adenocarcinoma cells express TRPM7 channel whose presence is essential for cell survival. The protein is a likely potential target for the pharmacological treatment of gastric cancer. (*Cancer Sci* 2008; 99: 2502–2509)

Ca^{2+} and Mg^{2+} have a fundamental role in countless cellular processes, including modulation of ion channels, receptors, G proteins, effector enzymes, cell proliferation, and survival.[1–3]

Among ion channels, the transient receptor potential (TRP) melastatin 6 and 7 channel is similarly permeable to both of the dominant divalent cations Ca^{2+} and Mg^{2+}.[4] TRP channels were first cloned from the *Drosophila* species (TRP and transient receptor potential–like protein) and constitute a superfamily of proteins that encode a diverse group of Ca^{2+}-permeable non-selective cation channels.[5] The TRP family is divided into three subfamilies: classic, vanilloid (TRPV), and melastatin type (TRPM).[5] The eight TRPM family members differ significantly from other TRP channels in terms of domain structure, cation selectivity, and activation mechanisms.[5] By mediating cation entry as well as membrane depolarization, activation of the TRPM subfamily of ion channels has a profound influence on various physiologic and pathologic processes.[6,7]

TRPM7 is endogenously expressed in a wide variety of tissues including brain and hematopoietic tissues[8] as well as kidney and heart tissues.[9–11] The TRPM7 cation channel supports multiple cellular and physiological functions, including cellular Mg^{2+} homeostasis,[12,13] cell viability and growth,[13–16] anoxic neuronal cell death,[17] synaptic transmission,[18] cell adhesion,[19,20] and intestinal pacemaking.[21] Recently, Wykes *et al*.[22] suggested that TRPM7 channels are critical for human mast cell survival, and Jiang *et al*.[23] suggested that activation of TRPM7 channels is critical for the growth and proliferation of human head and neck carcinoma cells. Also Abed *et al*.[24] proposed the importance of TRPM7 in human osteoblast-like cell proliferation. However, the presence and potential function of TRPM7 channels in human gastric cancer cells are unknown.

In this study, we examined the presence and potential role of TRPM7 channels in the growth and survival of AGS cells, the most common human gastric adenocarcinoma cell line. Our data suggest that TRPM7 channels have an important role in the survival of these tumor cells.

Materials and Methods

Cells. Five human gastric adenocarcinoma cell lines (AGS, MKN-1, MKN-45, SNU-1, and SNU-484) were used. Among them, we used mainly AGS cell line, the most common human gastric adenocarcinoma cell line. All cell lines were established at the Cancer Research Center, College of Medicine, Seoul National University, Korea. All cell lines were propagated in RPMI-1640 medium (Gibco-BRL) supplemented with 10% heat-inactivated fetal bovine serum and 20 μg/mL penicillin and streptomycin in an atmosphere of 5% CO_2 at 37°C.

Patch-clamp experiments. Experiments were performed at room temperature (22–25°C) by using the whole-cell configuration of the patch-clamp technique. AGS cells were transferred to a small chamber on the stage of an inverted microscope (IX70; Olympus, Japan), and were constantly perfused with in a solution containing (mmol/L) KCl 2.8, NaCl 145, $CaCl_2$ 2, glucose 10, $MgCl_2$ 1.2, and HEPES 10, adjusted to pH 7.4 with NaOH. The pipette solution contained (mmol/L) Cs-glutamate 145, NaCl 8, Cs-2-bis(2-aminophenoxy)-ethane-*N*,*N*,*N*′,*N*′-tetraacetic acid 10, and HEPES-CsOH 10, adjusted to pH 7.2 with CsOH. An Axopatch I-D (Axon Instruments, Foster City, CA, USA) was used to amplify membrane currents and potentials. For data acquisition and the application of command pulses, pCLAMP software v.9.2 and Digidata 1322A (Axon Instruments) were used. Results were analyzed by using pClamp and Origin software (Microcal Origin version 6.0).

RNA preparation and reverse transcription–polymerase chain reaction (RT-PCR). Total RNA was extracted by using an RNeasy Mini Kit (Qiagen), and reverse transcription of total RNA was performed by using random hexamer primers and Superscript II-RT (Life Technologies), according to the manufacturer's instructions. PCR primers were as follows: the TRPM7 first PCR amplification with upstream primers (5′-CCATACCATATTCTCCAAGGTTCC-3′), and downstream primers (5′-CATTCCTCTTCAGATCTGGAAGTT-3′) was performed for 40 cycles under the following conditions: denaturing

[3]To whom correspondence should be addressed. E-mail:insuk@plaza.snu.ac.kr

doi: 10.1111/j.1349-7006.2008.00982.x

at 94°C for 2 min, annealing at 50°C for 1 minute, and polymerization at 72°C for 1 minute. Nested PCR amplifications with TRPM7 upstream primers (5′-GCTGTATTGCCATTCAGCAG-3′) and downstream primers (5′-TTCTCCTAGATTTGCTGGGC-3′) were performed for 40 cycles under the following conditions: denaturing at 94°C for 2 min, annealing at 50°C for 1 min, and polymerization at 72°C for 1 min. A primer pair for the detection of human β-actin was used as the internal control.

Sodium dodecyl sulfate–polyacrylamide gel electrophoresis western blotting. Western blotting was performed by using lysates of AGS cells. Proteins were separated by sodium dodecyl sulfate–polyacrylamide gel electrophoresis by using 6% or 8% polyacrylamide gels, transferred to a polyvinylidene difluoride membrane, and analyzed by anti-TRPM7 (1:1000) and anti-PARP (1:500) antibodies. All procedures used standard methods.

Immunocytochemistry. AGS cells were seeded on coverslips precoated with poly-L-lysine (Sigma) for 24 h. The cells on the coverslips were fixed with 4% paraformaldehyde for 15 min and permeabilized with 0.1% Triton/phosphate-buffered saline (PBS) for 15 min at room temperature. After rinsing in PBS several times, the AGS cells were pre-incubated for 30 min with 1% skim milk and then they were incubated successively with 1:500 diluted TRPM7 antiserum overnight at 4°C and with fluorescein isothiocyanate (FITC)–labeled antirabbit chicken antiserum (Molecular Probes) for 1 h after washing with PBS. The coverslips were sealed with anti-quenching solution (GEL/MOUNT; Pleasanton, CA, USA) to prevent evaporation. Immunostained cells were observed under a confocal laser scanning microscope (FV500; Olympus) equipped with an argon/krypton laser source.

RNA interference. All the synthetic siRNAs were designed at Qiagen using the BIOPREDsi algorithm licensed from Novartis. All siRNA target sequences for silencing of the *TRPM7* gene (GenBank accession number NM_017672) were as follows: TRPM7siRNA1-5′-CCTGTAAGATCTATCGTTCAA-3′; TRPM7-siRNA2-5′-CTGCTAGCGTATATTCATAAA-3′; and TRPM7-siRNA3-5′-CCCTGACGGTAGATACATTAA-3′. siRNA transfections were performed in 12-well plates. Transfection parameters were optimized prior to validation according to the instructions given in the HiPerFect Transfection Reagent handbook. A negative scrambled siRNA (Qiagen) was used to verify that the effect seen with TRPM7 siRNA was not due to the transfection process. Relative intensities of protein bands were analyzed with a GS-710 Image Densitometer (Bio-Rad Laboratories, Hercules, CA, USA).

MTT (3-[4,5-dimethylthiazol-2-yl]-2,5-diphenyltetrazolium bromide) assay. Cell viability was assessed by MTT assay. The AGS cells were seeded into each well of 12-well culture plates and then cultured in RPMI-1640 supplemented with other reagents for 72 h. After incubation, 100 μL of MTT solution (5 mg/mL in PBS) was added to each well, and the plates were then incubated for 4 h at 37°C. After removing the supernatant and shaking with 200 μL of dimethyl sulfoxide (Jersey Lab Supply, Livingston, NJ, USA) for 30 min, absorbance was measured at 570 nm. All experiments were repeated at least three times.

Flow cytometric analysis. In order to investigate whether the cell cycle of AGS cells was redistributed, flow cytometric analysis was used with propidium iodine (PI) stain.[25,26] 1×10^6 cells were placed in an e-tube. 700 μL of a ice-cold fixation buffer (ethyl alcohol) was slowly added with vortexing. Tubes were sealed with parafilm and incubated at 4°C overnight. Samples were spun for 3 min at 106 g at 4°C, and the supernatant was aspirated and discarded. The cell pellet was resuspended by 200 μL of PI staining solution (PI [5 mg/mL] 2 μL and RNase 2 μL in PBS 196 μL) at 20817 g for 5 s. After 30 min in the dark at room temperature, samples were analyzed in a fluorescence-activated cell sorter (FACScan; Becton-Dickinson, Moutain View, CA, USA) at $\lambda = 488$ nm using Cell-Quest software (Becton-Dickinson). The DNA content distribution of normal growing cells is characterized by two peaks, the G1/G0 and G2/M phases. The G1/G0 phase comprises the normal functioning and resting state of the cell cycle with the most diploid DNA content, while the DNA content in the G2/M phase is more than diploid. Cells in the sub-G1 phase have the least DNA content in cell cycle distribution; this is termed hypodiploid. The hypoploid DNA contents represent the DNA fragmentation.[26]

Caspase-3 assay. Caspase-3 assay kits (Cellular Activity Assay Kit Plus) were purchased from BioMol (Plymouth, PA, USA). After experimental treatment, cells were centrifuged (1000 *g*, 4°C, 10 min) and washed with PBS. Cells were resuspended in ice-cold cell lysis buffer and incubated on ice for 10 min. Sample were centrifuged at 10 000 *g* (4°C, 10 min), and the supernatant was removed. Supernatant samples (10 μL) were incubated with 50 μL of substrate (400-μM Ac-DEVD-pNA) in 40 μL of assay buffer at 37°C. Absorbance at 405 nm was read at several time-points. pNA concentration in samples was extrapolated from a standard created with absorbances of sequential pNA concentrations.

Statistical analysis. Data are expressed as mean ± SEM. Differences between the data were evaluated by Student's *t*-test. A *P*-value of 0.05 was taken to indicate a statistically significant difference. The *n*-values reported in the text refer to the number of cells used in the patch-clamp experiments.

Results

TRPM7-like current in AGS cells. To investigate electrophysiological characteristics in AGS cells, we performed whole-cell voltage-clamp recordings. From a holding potential of –60 mV, single steps of 100 ms duration were applied in 10 mV increments (–100 to +100 mV) with standard bath and with pipette solutions lacking MgATP. Immediately after obtaining the whole-cell configuration, no current was evident. An outward-rectifying current slowly developed over time with peak current amplitudes occurring 5–8 min after obtaining the whole-cell configuration ($n = 7$; Fig. 1A-a). This current displayed no notable inactivation over the duration of the pulse. The amplitude of the current then remained stable for the duration of the experiments (10–15 min). The mean peak inward and outward currents at –100 and +100 mV were -4.0 ± 1.0 pA/pF and 73.5 ± 5.3 pA/pF, respectively ($n = 8$). The current–voltage (I–V) curve from the same cell is shown in Fig. 1A-b. A voltage ramp from +100 mV to 100 mV evoked small inward currents at negative potentials, whereas larger outward currents were evoked at positive potentials, showing outward-rectifying cation currents ($n = 10$; Fig. 1B-a). After the current had stabilized in normal bath solution, a divalent-free solution was perfused into the bath, and this resulted in large inward and outward currents with little rectification ($n = 10$; Fig. 1B-a). These features are very similar to those associated with the recently cloned TRPM6 or TRPM7 channel.[4,12] Two closely related TRPM channel subtypes, TRPM6 and TRPM7, are activated by lowered intracellular Mg^{2+} and have similar biophysical properties including an outwardly rectifying I–V relationship, cation selectivity $P_{Na}/P_{Cl} = 1/0.06$, and divalent permeability.[27] TRPM7 is one of the ubiquitously expressed ion channels,[13,14,28,29] and TRPM6 is expressed in intestine and renal distal tubules.[4,10] Kozak and Cahalan found that MIC (or TRPM7) channels in rat basophilic leukemia cells were inhibited by internal divalent cations.[30] TRPM7-like current in rat brain microglia was also inhibited by the internal Mg^{2+}.[28] In Jurkat E6-1 human leukemic T cells, internal Mg^{2+} has been used as a tool to isolate the Ca^{2+} release–activated Ca^{2+} current from that of TRPM7 channels.[31] To provide evidence that the inhibition by internal Mg^{2+} is involved in this current, various internal Mg concentration was included in the pipette solution and the currents were recorded. Under the lower concentration, the amplitude of this current was indeed larger compared with higher concentration and the presence of internal 2-mmol/L Mg^{2+} significantly inhibited

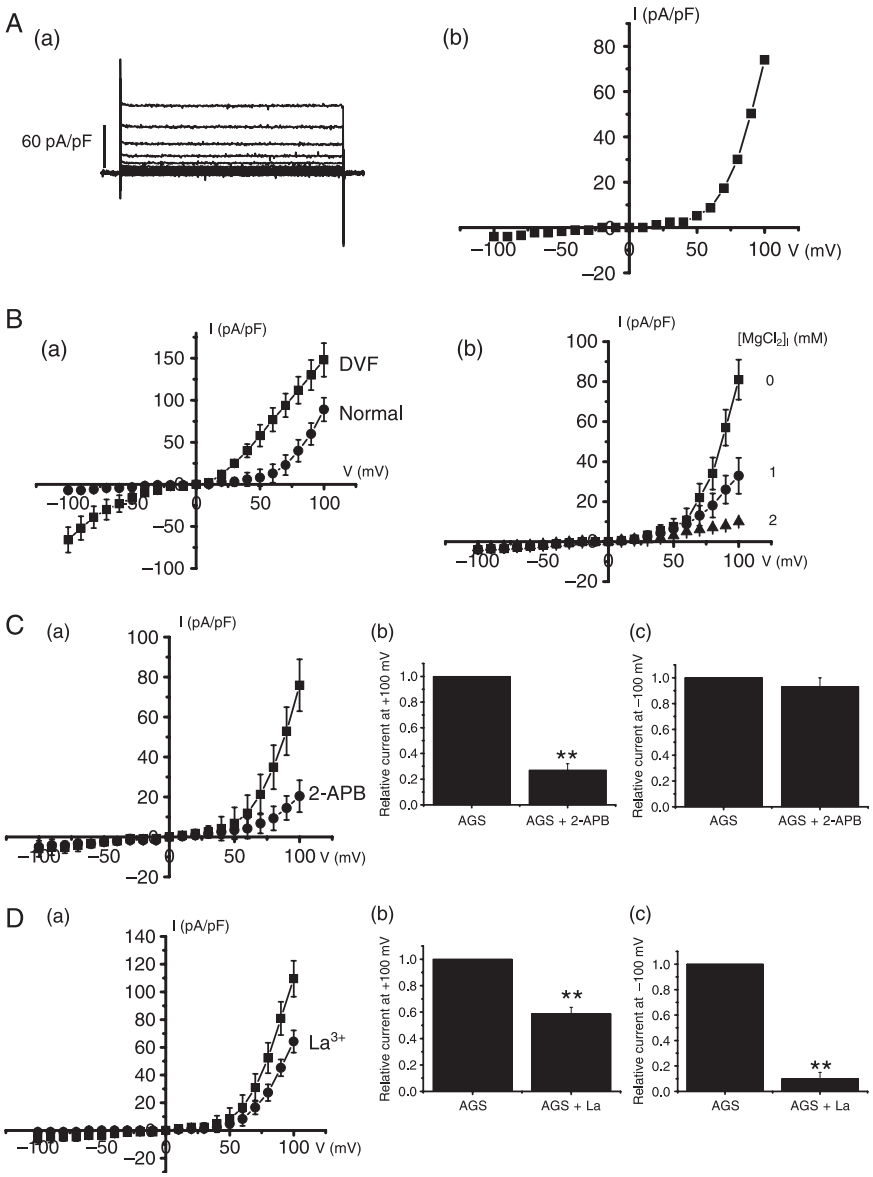

Fig. 1. Electrophysiologic and pharmacologic characteristics of transient receptor potential melastatin 7 (TRPM7)–like current in AGS cells. (A-a) From a holding potential of –60 mV, single steps of 100 ms duration were applied in 10 mV increments (–100 to +100 mV). An outward-rectifying current slowly developed over time with peak current amplitudes occurring 5–8 min after obtaining the whole-cell configuration. This current displayed no notable inactivation over the duration of the pulse. (A-b) I–V curve from the same cell is shown. Results are from representative AGS cells. (B-a) Representative TRPM7-like currents in AGS cells. A voltage ramp from –100 to +100 mV was applied from a holding potential of –60 mV (normal, ■). The complete removal of external divalents increases both inward and outward monovalent current flow with little rectification (divalent free [DVF], ●). (B-b) TRPM7-like currents in AGS cells at 0, 1, or 2 mmol/L $[Mg^{2+}]_i$. A voltage ramp from –100 to +100 mV was applied from a holding potential of –60 mV. (C) Effect of 2-APB on TRPM7-like current. I–V curves and summary bar graph in the absence (■) and presence (●) of 100-μmol/L 2-APB. (D) Effect of La^{3+} on TRPM7-like current. I–V curves and summary bar graph in the absence (■) and presence (●) of 100-μmol/L La^{3+}. $^{**}P < 0.01$.

this current ($n = 8$; Fig. 1B-b). The estimated median inhibitory concentration value for free Mg^{2+} was 560 μmol/L.

We investigated the various pharmacological effects of these currents in AGS cells. 2-APB has broad inhibitory effects on the TRP superfamily.[15,32–35] Also 2-APB is a useful tool for differentiating TRPM6 and TRPM7.[36] At micromolar concentrations, 2-APB enhanced TRPM6 but inhibited TRPM7 currents.[36] In the presence of 100-μmol/L 2-APB, the amplitude of the currents were inhibited by 72.9% ± 2.9% outwardly and 7.2% ± 3.9% inwardly ($n = 7$; Fig. 1C). The inhibition by 2-APB suggests that TRPM7 channels are involved in this current, and not TRPM6 channels. Also previous studies have shown that La^{3+} is a potent non-specific blocker for TRPM7 channels.[14] La^{3+} has been reported to completely block the inward, but to only partially block the outward, currents of cloned TRPM7 channels.[10] In the presence of 100-μmol/L La^{3+} in the bath solution, the outward current was partially inhibited by 41.3% ± 4.9% and the inward current inhibited by 90.1% ± 5.2% ($n = 8$; Fig. 1D).

Taken together, both electrophysiologic and pharmacologic data indicate that these currents in AGS cells are TRPM7-like currents.

Detection of TRPM7 mRNA and protein in human gastric adenocarcinoma cell lines. To reinforce the existence of TRPM7 channels, biochemical and molecular biological techniques were used. As shown in Fig. 2a, RT-PCR detected the presence of TRPM7 mRNA in human gastric adenocarcinoma cell lines. Western blotting showed a clear band of ~220 kDa of TRPM7 proteins (Fig. 2b). To verify the specificity of the antibody used, HEK293 cells with inducible expression of TRPM7 were used as a positive control.[14] Following induction of TRPM7 expression, a clear protein band of ~220 kDa was detected in HEK293 cells (Fig. 2b). Also, expression of TRPM7 proteins was investigated by immunoreactivity in AGS cells (Fig. 2c).

Effects of TRPM7 siRNA in AGS cells. For determination that this TRPM7-like current was really mediated by activation of TRPM7 channel, we used RNA interference (RNAi). To prevent non-specific effects of the small interfering RNA (siRNA) sequence used, we generated three types of 21-nucleotide siRNA specifically targeting human TRPM7, that is, TRPM7siRNA1, TRPM7siRNA2, and TRPM7siRNA3 (see 'Materials and Methods'). In our experiments, ~90% of AGS cells were successfully transfected with siRNA, as indicated by FITC fluorescence. In AGS cells transfected by TRPM7siRNA, we could see a relative molecular mass of 220 kDa by western blotting. As seen in Fig. 3a, TRPM7siRNA1 had no effect on TRPM7 protein expression,

doi: 10.1111/j.1349-7006.2008.00982.x

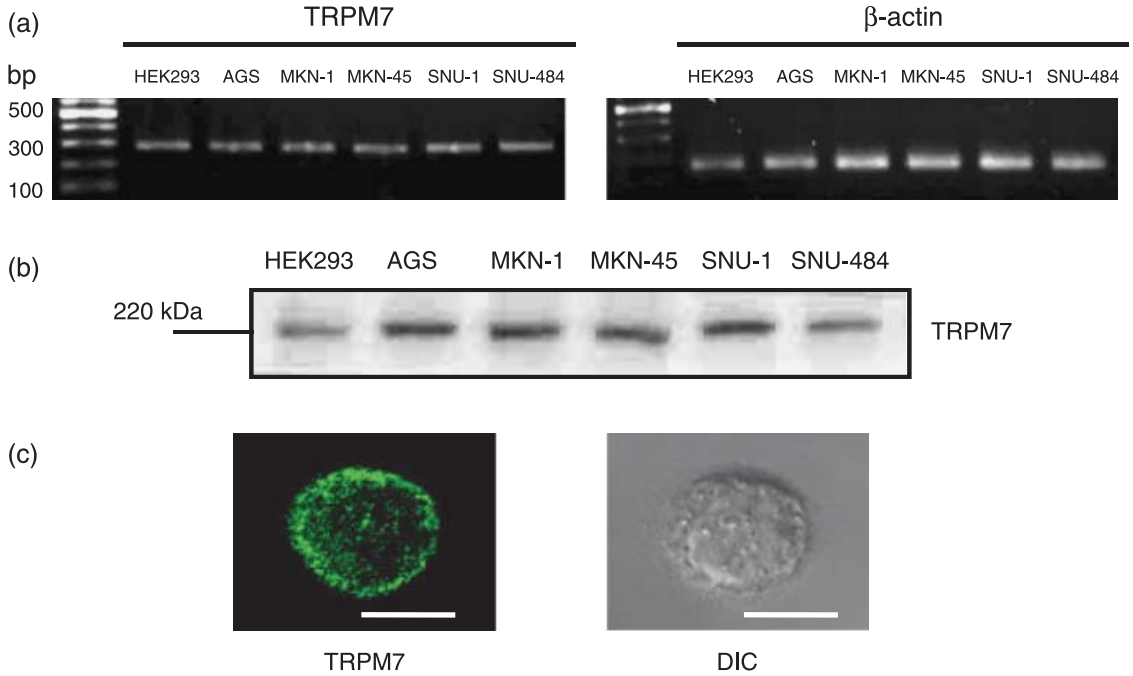

Fig. 2. Detection of transient receptor potential melastatin 7 (TRPM7) mRNA and protein in human gastric adenocarcinoma cell lines. (a) Reverse transcrption–polymerase chain reaction detection of TRPM7 mRNA in human gastric adenocarcinoma cell lines. HEK293 cells with inducible expression of TRPM7 served as a positive controls and β-actin was used as an internal control. (b) TRPM7 proteins were detected at molecular weight 220 kDa by western blotting. HEK293 cells with inducible expression of TRPM7 served as a positive control. (c) TRPM7 immunoreactivity in AGS cell under confocal microscopy (left) and its differential interference contrast image (right). Horizontal bar indicates 10 μm.

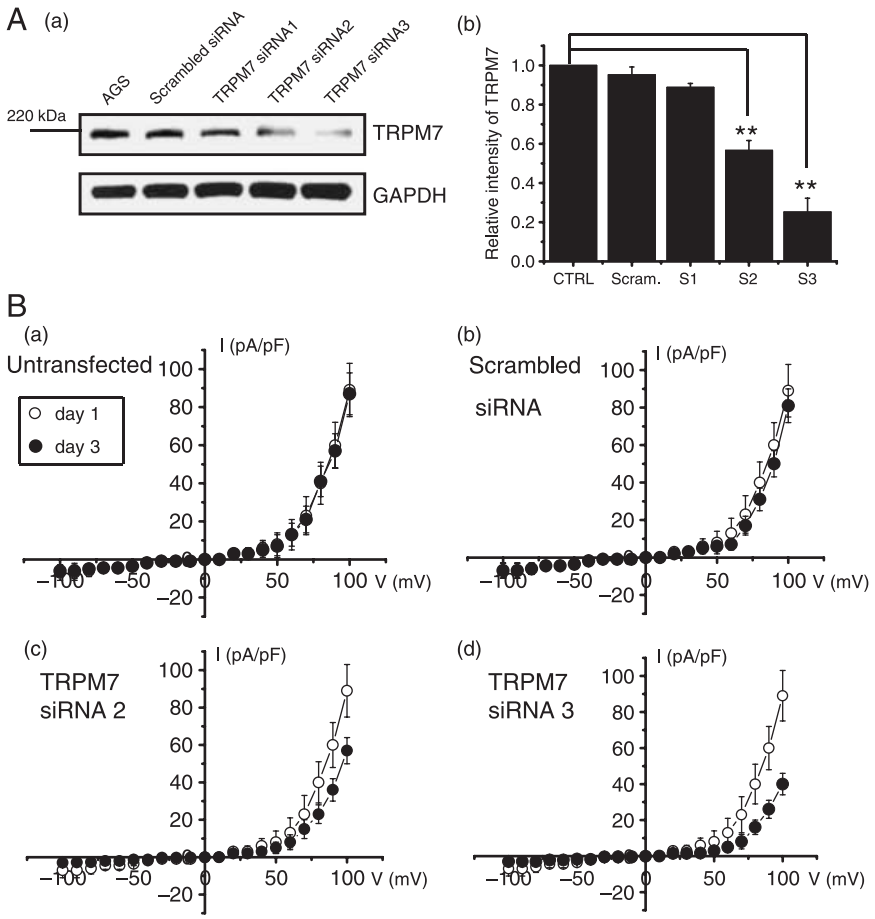

Fig. 3. Effect of transient receptor potential melastatin 7 (TRPM7) RNAi in AGS cells. (A-a) Sodium dodecyl sulfate–polyacrylamide gel electrophoresis analysis of TRPM7 RNAi effects on AGS cells. RNAi effects are shown (TRPM7siRNA2 and TRPM7siRNA3). Glyceraldhyde-3-phosphate dehydrogenase (GAPDH) was used as an internal control. (A-b) Densitometric analysis of TRPM7 protein expression presented in (A) ($n = 5$). CTRL, AGS cells; Scram, scrambled siRNA; S1, TRPM7siRNA1; S2, TRPM7siRNA2; S3, TRPM7siRNA3. Values are mean ± SEM. $^{**}P < 0.01$. (B) The RNAi-mediated reduction in TRPM7-like currents. TRPM7-like currents were markedly reduced at 72 h after transfection with TRPM7siRNA3 but not with scrambled siRNA. Mean data from experiments performed on separate occasions ($n = 6$, respectively).

and TRPM7siRNA2 suppressed TRPM7 protein expression only to a moderate degree. Significantly, TRPM7siRNA3 silenced TRPM7 protein expression by 70–80% without reducing the expression of glyceraldhyde-3-phosphate dehydrogenase (GAPDH).

To confirm that the siRNAs had reduced TRPM7 protein expression, cells were also analyzed using electrophysiology. Patch-clamp recording was done at 72 h after TRPM7 siRNA transfection. As shown in Fig. 3b, the amplitude of TRPM7-like currents was significantly reduced in AGS cells transfected with TRPM7siRNA3 when compared with the scrambled control. Thus at +100 mV, outward currents were 81.1 ± 9.2 pA/pF in scrambled controls ($n = 6$) at 72 h after transfection, compared with 40.3 ± 6.5 pA/pF for TRPM7siRNA3 ($P < 0.01$) ($n = 6$). Transfection with the scrambled siRNA control had no effect on TRPM7 currents (Fig. 3b).

Inhibition of cell survival by TRPM7 blockade and TRPM7siRNA. TRPM7 has been proposed as a requirement for cell survival on the basis of experiments in genetically engineered DT-40 B-cells.[14] Recently, Wykes *et al*.[22] suggested that TRPM7 is critical for human mast cell survival. Therefore, we investigated whether the activities of TRPM7 channels influence the survival of AGS cells. First, we tested the effect of 2-APB, a non-specific TRPM7 channel inhibitor, on the survival of AGS cells. Addition of 10, 50, 100 μmol/L, and 1 mmol/L 2-APB in the culture medium inhibited the survival of AGS cells by 22.1% ± 2.1%, 40.2% ± 1.6%, 60.5% ± 2.1%, and 96.1% ± 1.4% with MTT assay ($n = 5$; Fig. 4a). Similar to 2-APB, La^{3+} also inhibited the survival of AGS cells ($n = 5$; Fig. 4b).

TRPM7siRNA was used to selectively suppress the expression of TRPM7 channels. As shown in Fig. 4c, there was significant cell death in AGS cells transfected with TRPM7siRNA3 by 54.4% ± 3.8% with the MTT assay. Cells transfected with control scrambled siRNA showed no difference in cell survival compared to non-transfected cells. Taken together, our data suggest that activation of TRPM7 channels plays an important role in the survival of AGS cells.

Inhibition of TRPM7 channels lead to increased apoptosis. To determine whether AGS cell death occurred by apoptosis, we used sub-G1 analysis, and the method of specific proteolytic cleavage of the DNA repair enzyme, poly (ADP-ribose) polymerase (PARP). As a method to analyze the mode of cell death in AGS cells transfected with TRPM7siRNA, we used sub-G1 analysis.[37,38] In this protocol, transfected cells are stained with a fluorescent DNA stain (such as PI). Due to the action of endogenous endonucleases in apoptotic cells, the DNA is cleaved into endonucleosomal fragments of typical sizes. These DNA fragments are extracted from the cells. This loss of DNA is detectable by FACS analysis, as the reduced nuclear staining of apoptotic cells results in a novel (sub-G1) fluorescence peak to the left of the regular fluorescence peak. The sub-G1 in TRPM7siRNA3 was markedly increased by 29.2% ± 3.7%; Fig. 5a). Caspase-3

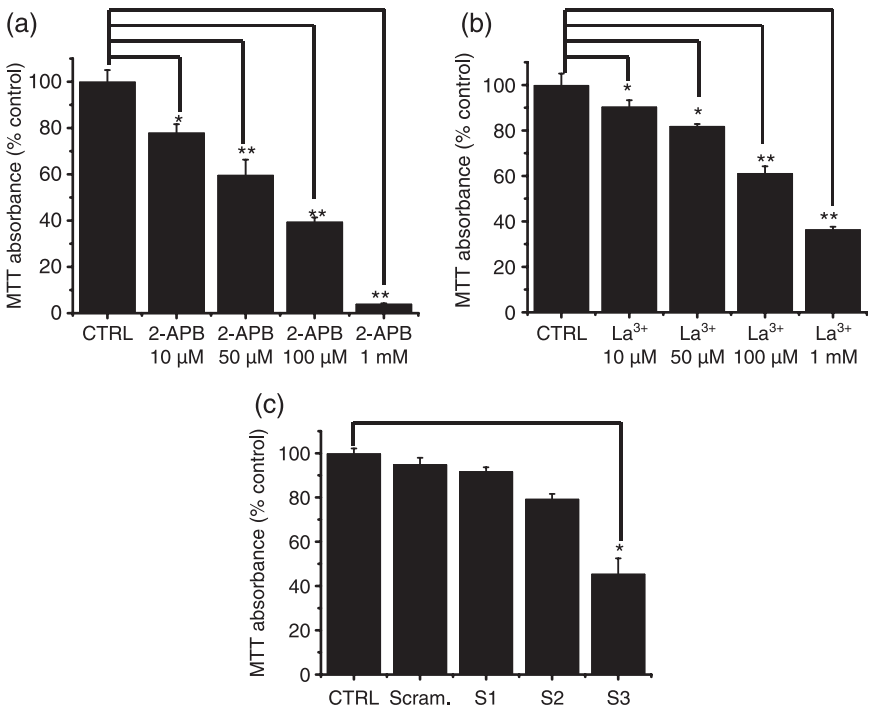

Fig. 4. Effect of 2-APB, La^{3+}, and RNAi on cell viability with a MTT (3-[4,5-dimethylthiazol-2-yl]-2,5-diphenyltetrazolium bromide)–based viability assay. (a,b) Cell viability was significantly decreased at high concentrations of 2-APB and La^{3+}. (c) Cell viability was decreased at 72 h after transfection with TRPM7siRNA3. CTRL, AGS cells; Scram, scrambled siRNA; S1, TRPM7siRNA1; S2, TRPM7siRNA2; S3, TRPM7siRNA3. Values are mean ± SEM. $*P < 0.05$. $**P < 0.01$.

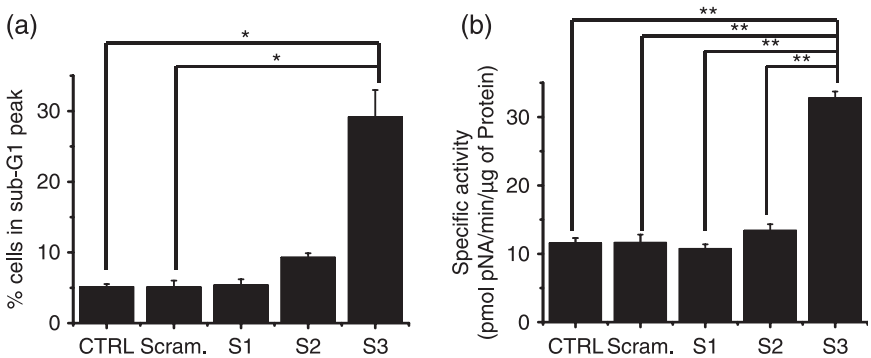

Fig. 5. Inhibition of transient receptor potential melastatin 7 (TRPM7) channels lead to increased apoptosis. (a) Sub-G1 peak measured by FACScan. Quantitative data of three independent experiments. (b) Caspase-3 activities measured by enzyme assays. The specific activity was obtained from three samples per group. CTRL, AGS cells; Scram, scrambled siRNA; S1, TRPM7siRNA1; S2, TRPM7siRNA2; S3, TRPM7siRNA3. $*P < 0.05$. $**P < 0.01$.

doi: 10.1111/j.1349-7006.2008.00982.x

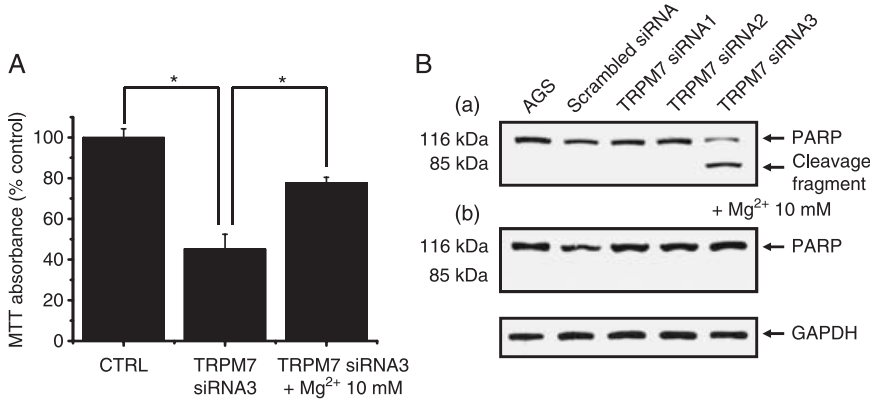

Fig. 6. Mg^{2+} involvement in cell death. (A) Cell viability was decreased at 72 h after transfection with transient receptor potential melastatin 7 (TRPM7) siRNA3, but in the case of supplementing their growth media with 10 mmol/L Mg^{2+}, cell viability decreased little. Values are mean ± SEM. *$P < 0.05$. (B) A representative western blotting of transfected cells with anti-PARP antibody. Cells transfected with TRPM7siRNA3 represent increased PARP cleavage, but there was no cleavage when supplementing 10 mmol/L Mg^{2+}. Glyceraldhyde-3-phosphate dehydrogenase (GAPDH) was used as an internal control.

activation is one of the hallmarks of apoptotic cell death.[39] We measured the enzyme activity in AGS cells transfected with TRPM7siRNA. Using a synthetic substrate, we found caspase-3 activity in AGS cells to be 11.5 ± 0.7 nmol pNA/min/μg protein. In AGS cells, after 72-h transfection with TRPM7siRNA3, elevated caspase-3 activity was 32.8 ± 0.9 nmol pNA/min/μg protein ($P < 0.01$; Fig. 5b). We further characterized the changes in caspase-3 activity by western blotting analysis of its natural substrate, the PARP. PARP has been shown to be a cellular target of caspase-3 and other caspases. During apoptosis, PARP becomes proteolytically cleaved from a 116-kDa-intact form into 85 and 25 kDa fragments. Caspase-3 cleaves a 116-kDa fragment from PARP, and a second band corresponding to the 85-kDa fragment appears in the western blot. In AGS cells, after 72-h transfection with TRPM7siRNA3, PARP cleavage was increased. (Fig. 6B-a).

Mg^{2+} involvement in cell death. TRPM7 permeates Mg^{2+} and TRPM7 plays a critical role in cellular Mg^{2+} homeostasis.[12,14] A recent study has indicated that the growth defect in TRPM7-deficient cells could be rescued by supplemental Mg^{2+}.[12] In this study we investigated whether the cell death in AGS cells transfected with TRPM7siRNA3 could be ameliorated to any extent by supplementing their growth media with Mg^{2+}. As shown in Fig. 6A, provision of 10 mmol/L supplemental Mg^{2+} allowed the survival and growth of AGS cells. In the caspase-3 activity test, there was no cleavage fragment of its natural substrate, the PARP (Fig. 6B-b)

Discussion

Ion channels have an important role in a wide variety of biological processes that involve in excitability, gene expression, muscle contraction, cell volume regulation, hormone secretion, etc. In addition to these life-supporting activities, ion channels are also associated with several diseases.[40,41] Over the past 10 years, ion channels have been crucial for tumor development and growth of cancer. When epithelial cells change from being normal to being cancerous, a series of genetic alterations occur, which may also affect the expression of ion channels or cause a change in ion channel activity.[42] Voltage-gated potassium ion channels were overexpressed in colon cancer[43] and voltage-gated sodium ion channels were involved in the growth of prostate cancer.[44] Volume-regulated Cl^- channels were found in a human prostate cancer cell line and in lung cancer cells.[45,46] TRP proteins have diverse functional properties and profound effects on a variety of physiological and pathological conditions. TRPV6 is overexpressed in prostate adenocarcinoma and is a promising target for new therapeutic strategies for the treatment of advanced prostate cancer.[47] The down-regulation of TRPM1 transcript expression in human cutaneous melanoma appears to be a prognostic marker for melanoma metastasis.[48] In addition, TRPM8 channel protein has been used as a prostate-specific marker and the loss of TRPM8 is considered as a sign of poor prognosis.[49,50] Recently, Jiang *et al.*[23] suggested that activation of TRPM7 channels is critical for the growth and proliferation of human head and neck carcinoma cells. Therefore, the research into the pathophysiologic function of ion channels is one of the interesting areas that may offer alternative prognostic and therapeutic strategies for cancer patients. In line with this argument, our studies showed that activation of TRPM7 channels influence the growth and survival of human gastric adenocarcinoma cells.

Several line of evidence indicate that this current is carried, at least partially, by TRPM7 channels. (1) Whole-cell voltage-clamp recordings revealed that TRPM7-like currents have strong outward rectification of the current–voltage relationship, modulated by intracellular Mg^{2+}, and inhibited by external 2-APB and La^{3+} (Fig. 1). This feature is similar to TRPM7 currents recorded in other cells and in heterologous expression systems.[14,17,28,31] (2) RT-PCR, western blot, and immunoreactivity detected the presence of TRPM7 mRNA and protein (Fig. 2). (3) Reduction of the current by TRPM7 siRNA supports the involvement of TRPM7 channels (Fig. 3).

TRPM7 is a member of the transient receptor potential melastatin subfamily of ion channels. It is very closely related to TRPM6 with which it shares very similar electrophysiological properties and an α-kinase domain in the C terminus. Although both channels are apparently involved in Mg^{2+} homeostasis, and can potentially form TRPM6/7 heterodimers, they have also been shown to have non-redundant roles.[51] However, there are biophysical differences between the two channels, including a differential response of TRPM7 to the inositol triphosphate (IP_3) inhibitor 2-APB. Micromolar levels of 2-APB increase TRPM6 but significantly inhibit TRPM7 channel activities.[52] In AGS cells, these currents were inhibited by micromolar levels of 2-APB. Therefore, TRPM6 does not play an important role in this system.

TRPM7 plays a critical role in cellular Mg^{2+} homeostasis[12] and cortical-neuronal cell death in response to oxygen and glucose deprivation–induced stress.[17] In AGS cells, there was significant cell death in cells transfected with TRPM7siRNA. But in the case of receiving 10-mM supplemental Mg^{2+}, cells transfected with TRPM7siRNA were able to grow. Therefore, in AGS cells Mg^{2+} may be one of the important keys in cell growth and survival.

Some have described that Mg deprivation induces cell death by apoptosis, for example in primary cultures of rat hepatocytes.[53] They concluded that Mg deficiency provoked apoptotic death by an increased susceptibility to oxidative stress. Dietary Mg restriction in rats also accelerated thymus involution, a typical example of apoptosis,[54] although in this case the inflammatory process could be a confounding factor.

Apoptotic cell death pathways are induced by a variety of signals. One mechanism which is consistently implicated in apoptosis is the activation of a series of cytosolic proteases, the caspases.[55] Caspases are synthesized as inactive proenzymes that are processed in cells undergoing apoptosis by self-proteolysis and/or cleavage by another protein. Functionally, active caspases form a proteolytic cascade, capable of cleaving and activating specific substrates, including an enzyme involved in DNA repair and genomic maintenance, PARP. Such cleavage events may result in important alterations to normal homeostatic cellular processes.[56] PARP has been shown to be a cellular target of caspase-3 and other caspases. In AGS cells, after 72-h transfection with TRPM7siRNA, PARP becomes proteolytically cleaved from a 116-kDa intact form into 85-kDa fragments (Fig. 6B) and caspase-3 activity is increased (Fig. 5b).

In summary we have demonstrated that human gastric adenocarcinoma cells express functional TRPM7 channels that are involved, at least partially, in cell growth and survival.

Acknowledgments

This work was supported by the Creative Research Initiative Center for Bio-Artificial Muscle of the Ministry of Science and Technology (MOST) and the Korea Science and Engineering Foundation (KOSEF).

References

1 Berridge MJ, Lipp P, Bootman MD. The versatility and universality of calcium signaling. *Nat Rev Mol Cell Biol* 2000; **1**: 11–21.
2 Romani AM, Scarpa A. Regulation of cellular magnesium. *Front Biosci* 2000; **5**: D720–34.
3 Volpe P, Vezu L. Intracellular magnesium and inositol 1,4,5-trisphosphate receptor: molecular mechanisms of interaction, physiology and pharmacology. *Magnes Res* 1993; **6**: 267–74.
4 Voets T, Nilius B, Hoefs S *et al*. TRPM6 forms the Mg^{2+} influx channel involved in intestinal and renal Mg^{2+} absorption. *J Biol Chem* 2004; **279**: 19–25.
5 Clapham DE. TRP channels as cellular sensors. *Nature* 2003; **426**: 517–24.
6 Ramsey IS, Delling M, Clapham DE. An introduction to TRP channels. *Annu Rev Physiol* 2006; **68**: 619–47.
7 Minke B. TRP channels and Ca^{2+} signaling. *Cell Calcium* 2006; **40**: 261–75.
8 Minke B, Cook B. TRP channel proteins and signal transduction. *Physiol Rev* 2002; **82**: 429–72.
9 Montell C. The TRP superfamily of cation channels. *Sci STKE* 2005; **272**: re3.
10 Runnels LW, Yue L, Clapham DE. TRP-PLIK, a bifunctional protein with kinase and ion channel activities. *Science* 2001; **291**: 1043–7.
11 Montell C, Birnbaumer L, Flockerzi V. The TRP channels, a remarkably functional family. *Cell* 2002; **108**: 595–8.
12 Schmitz C, Perraud AL, Johnson CO *et al*. Regulation of vertebrate cellular Mg^{2+} homeostasis by TRPM7. *Cell* 2003; **114**: 191–200.
13 He Y, Yao G, Savoia C, Touyz RM. Transient receptor potential melastatin 7 ion channels regulate magnesium homeostasis in vascular smooth muscle cells: role of angiotensin II. *Circ Res* 2005; **96**: 207–15.
14 Nadler MJ, Hermosura MC, Inabe K *et al*. LTRPC7 is a Mg.ATP-regulated divalent cation channel required for cell viability. *Nature* 2001; **411**: 590–5.
15 Hanano T, Hara Y, Shi J *et al*. Involvement of TRPM7 in cell growth as a spontaneously activated Ca^{2+} entry pathway in human retinoblastoma cells. *J Pharmacol Sci* 2004; **95**: 403–19.
16 Elizondo MR, Arduini BL, Paulsen J *et al*. Defective skeletogenesis with kidney stone formation in dwarf zebrafish mutant for trpm7. *Curr Biol* 2005; **15**: 667–71.
17 Aarts M, Iihara K, Wei WL *et al*. A key role for TRPM7 channels in anoxic neuronal death. *Cell* 2003; **115**: 863–77.
18 Krapivinsky G, Mochida S, Krapivinsky L, Cibulsky SM, Clapham DE. The TRPM7 ion channel functions in cholinergic synaptic vesicles and affects transmitter release. *Neuron* 2006; **52**: 485–96.
19 Clark K, Langeslag M, van Leeuwen B *et al*. TRPM7, a novel regulator of actomyosin contractility and cell adhesion. *EMBO J* 2006; **25**: 290–301.
20 Su D, May JM, Koury MJ, Asard H. Human erythrocyte membranes contain a cytochrome b561 that may be involved in extracellular ascorbate recycling. *J Biol Chem* 2006; **281**: 39852–9.
21 Kim BJ, Lim HH, Yang DK *et al*. Melastatin-type transient receptor potential channel 7 is required for intestinal pacemaking activity. *Gastroenterology* 2005; **129**: 1504–17.
22 Wykes RC, Lee M, Duffy SM, Yang W, Seward EP, Bradding P. Functional transient receptor potential melastatin 7 channels are critical for human mast cell survival. *J Immunol* 2007; **179**: 4045–52.
23 Jiang J, Li MH, Inoue K, Chu XP, Seeds J, Xiong ZG. Transient receptor potential melastatin 7-like current in human head and neck carcinoma cells: role in cell proliferation. *Cancer Res* 2007; **67**: 10929–38.
24 Abed E, Moreau R. Importance of melastatin-like transient receptor potential 7 and cations (magnesium, calcium) in human osteoblast-like cell proliferation. *Cell Prolif* 2007; **40**: 849–65.
25 Nicoletti I, Migliorati G, Pagliacci MC, Grignani F, Riccardi C. A rapid and simple method for measuring thymocyte apoptosis by propidium iodide staining and flow cytometry. *J Immunol Methods* 1991; **139**: 271–9.
26 Wang BJ, Won SJ, Yu ZR, Su CL. Free radical scavenging and apoptotic effects of cordycepin sinensis ractionated by supercritical carbon dioxide. *Food Chem Toxicol* 2005; **43**: 543–52.
27 Kraft R, Harteneck C. The mammalian melastatin-related transient receptor potential cation channels: an overview. *Pflugers Arch* 2005; **451**: 204–11.
28 Jiang X, Newell EW, Chlichter LC. Regulation of a TRPM7-like current in rat brain microglia. *J Biol Chem* 2003; **278**: 42867–76.
29 Gwanyanya A, Sipido KR, Vereecke J, Mubagwa K. ATP and PIP_2 dependence of the magnesium-inhibited, TRPM7-like cation channel in cardiac myocytes. *Am J Physiol* 2006; **291**: 627–35.
30 Kozak JA, Cahalan MD. MIC channels are inhibited by internal divalent cations but not ATP. *Biophys J* 2003; **84**: 922–7.
31 Prakriya M, Lewis RS. Separation and characterization of currents through store-operated CRAC channels and Mg^{2+}-inhibited cation (MIC) channels. *J Gen Physiol* 2002; **119**: 487–507.
32 Xu SZ, Zeng F, Boulay G, Grimm C, Harteneck C, Beech DJ. Block of TRPC5 channels by 2-aminoethoxydiphenyl borate: a differential, extracellular and voltage-dependent effect. *Br J Pharmacol* 2005; **145**: 405–14.
33 Ma HT, Patterson RL, van Rossum DB, Birnbaumer L, Mikoshiba K, Gill DL. Requirement of the inositol trisphosphate receptor for activation of store-operated Ca^{2+} channels. *Science* 2000; **287**: 1647–51.
34 Schindl R, Kahr H, Graz I, Groschner K, Romanin C. Store depletion-activated CaT1 currents in rat basophilic leukemia mast cells are inhibited by 2-aminoethoxydiphenyl borate. Evidence for a regulatory component that controls activation of both CaT1 and CRAC (Ca^{2+} release-activated Ca^{2+}) channels. *J Biol Chem* 2002; **277**: 26950–8.
35 Trebak M, Bird GS, McKay RR, Putney JW Jr. Comparison of human TRPC3 channels in receptoractivated and store-operated modes. Differential sensitivity to channel blockers suggests fundamental differences in channel composition. *J Biol Chem* 2002; **277**: 21617–23.
36 Monteilh-Zoller MK, Hermosura MC, Nadler MJ, Scharenberg AM, Penner R, Fleig A. TRPM7 provides an ion channel mechanism for cellular entry of trace metal ions. *J Gen Physiol* 2003; **121**: 49–60.
37 Hotz MA, Gong J, Traganos F, Darzynkiewicz Z. Flow cytometric detection of apoptosis: comparison of the assays of in situ DNA degradation and chromatin changes. *Cytometry* 1994; **15**: 237–44.
38 Vermes I, Haanen C, Reutelingsperger C. Flow cytometry of apoptotic cell death. *J Immunol Methods* 2000; **243**: 167–90.
39 Faleiro L, Kobayashi R, Fearnhead H, Lazebnik Y. Multiple species of CPP32 and Mch2 are the major active caspases present in apoptotic cells. *EMBO J* 1997; **16**: 2271–81.
40 Pardo LA, Contreras-Jurado C, Zientkowska M, Alves F, Stühmer W. Role of voltage-gated potassium channels in cancer. *J Membr Biol* 2005; **205**: 115–24.
41 Bodding M. TRP proteins and cancer. *Cell Signal* 2007; **19**: 617–24.
42 Kunzelmann K. Ion channels and cancer. *J Membr Biol* 2005; **205**: 159–73.
43 Abdul M, Hoosein N. Voltage-gated potassium ion channels in colon cancer. *Oncol Rep* 2002; **9**: 961–4.
44 Abdul M, Hoosein N. Voltage-gated sodium ion channels in prostate cancer: expression and activity. *Anticancer Res* 2002; **22**: 1727–30.
45 Jirsch J, Deeley RG, Cole SP, Stewart AJ, Fedida D. Inwardly rectifying K^+ channels and volume-regulated anion channels in multidrug-resistant small cell lung cancer cells. *Cancer Res* 1993; **53**: 4156–60.
46 Shuba YM, Prevarskaya N, Lemonnier L *et al*. Volume regulated chloride conductance in the LNCaP human prostate cancer cell line. *Am J Physiol Cell Physiol* 2000; **279**: C1144–54.
47 Fixemer T, Wissenbach U, Flockerzi V, Bonkhoff H. Expression of the Ca^{2+}-selective cation channel TRPV6 in human prostate cancer: a novel prognostic marker for tumor progression. *Oncogene* 2003; **22**: 7858–61.
48 Duncan LM, Deeds J, Hunter J *et al*. Down-regulation of the novel gene melastatin correlates with potential for melanoma metastasis. *Cancer Res* 1998; **58**: 1515–20.
49 Tsavaler L, Shapero MH, Morkowski S, Laus R. Trpp8, a novel prostate-specific gene, is up-regulated in prostate cancer and other malignancies and

doi: 10.1111/j.1349-7006.2008.00982.x

shares high homology with transient receptor potential calcium channel proteins. *Cancer Res* 2001; **61**: 3760–9.
50 Henshall SM, Afar DE, Hiller J *et al*. Survival analysis of genome-wide gene expression profiles of prostate cancers identifies new prognostic targets of disease relapse. *Cancer Res* 2003; **63**: 4196–203.
51 Schmitz C, Dorovkov MV, Zhao X, Davenport BJ, Ryazanov AG, Perraud AL. The channel kinases TRPM6 and TRPM7 are functionally nonredundant. *J Biol Chem* 2005; **280**: 37763–71.
52 Li M, Jiang J, Yue L. Functional characterization of homo- and heteromeric channel kinases TRPM6 and TRPM7. *J Gen Physiol* 2006; **127**: 525–37.
53 Martin H, Richert L, Berthelot A. Magnesium deficiency induces apoptosis in primary cultures of rat hepatocytes. *J Nutr* 2003; **133**: 2505–11.
54 Malpuech-Brugère C, Nowacki W, Gueux E *et al*. Accelerated thymus involution in magnesium-deficient rats is related to enhanced apoptosis and sensitivity to oxidative stress. *Br J Nutr* 1999; **81**: 405–11.
55 Patel T, Gores GJ, Kaufmann SH. The role of proteases during apoptosis. *FASEB J* 1996; **10**: 587–97.
56 Lin C, Holland RE Jr, Donofrio JC, McCoy MH, Tudor LR, Chambers TM. Caspase activation in equine influenza virus induced apoptotic cell death. *Vet Microbiol* 2002; **84**: 357–65.